Bifunctional inhibitors of the trypsin-like activity of eukaryotic proteasomes

Günther Loidl, Michael Groll, Hans-Jürgen Musiol, Lars Ditzel, Robert Huber and Luis Moroder

Background: The 20S proteasome is a multicatalytic protease complex that exhibits trypsin-like, chymotrypsin-like and post-glutamyl-peptide hydrolytic activities associated with the active sites of the β2, β5 and β1 subunits, respectively. Modulation of these activities using inhibitors is essential for a better understanding of the proteasome's mechanism of action. Although there are highly selective inhibitors of the proteasome's chymotryptic activity, inhibitors of similar specificity have not yet been identified for the other activities.

Results: The X-ray structure of the yeast proteasome reveals that the sidechain of Cys118 of the β3 subunit protrudes into the S3 subsite of the β2 active site. The location of this residue was exploited for the rational design of bidentated inhibitors containing a maleinimide moiety at the P3 position for covalent linkage to the thiol group and a carboxy-terminal aldehyde group for hemiacetal formation with the Thr1 hydroxyl group of the active site. Structure-based modelling was used to determine the optimal spacing of the maleinimide group from the P2–P1 dipeptide aldehydes and the specificity of the S1 subsite was exploited to limit the inhibitory activity to the β2 active site. X-ray crystallographic analysis of a yeast proteasome–inhibitor adduct confirmed the expected irreversible binding of the inhibitor to the P3 subsite.

Conclusions: Maleoyl-β-alanyl-valyl-arginal is a new type of inhibitor that is highly selective for the trypsin-like activity of eukaryotic proteasomes. Despite the reactivity of the maleinimide group towards thiols, and therefore the limited use of this inhibitor for *in vitro* studies, it might represent an interesting new biochemical tool.

Address: Max-Planck-Institut für Biochemie, 82152 Martinsried, Germany.

Correspondence: Luis Moroder
E-mail: moroder@biochem.mpg.de

Key words: eukaryotic proteasome, selective inhibition, trypsin-like activity, X-ray analysis

Received: **13 November 1998**
Revisions requested: **4 January 1999**
Revisions received: **15 January 1999**
Accepted: **20 January 1999**

Published: **11 March 1999**

Chemistry & Biology April 1999, **6**:197–204
http://biomednet.com/elecref/1074552100600197

Introduction

The proteasome is a multicatalytic proteinase complex that is responsible for the intracellular protein turnover in prokaryotes and eukaryotes. This cellular function is linked to the protein degradation pathway that requires ubiquitin and ATP, involving the 26S proteasome in which the core and proteolytic chamber is formed by the 20S proteasome. The proteasome removes abnormal, misfolded or improperly assembled proteins from the cell and it is involved in the stress response, cell-cycle control, cell differentiation and metabolic adaptation to the cellular immune response [1–8].

The determination of the crystal structure of the 20S proteasome from *Saccharomyces cerevisiae* reveals that the 28 protein subunits are arranged as a $(\alpha1–\alpha7, \beta1–\beta7)_2$ complex consisting of four stacked rings [9]. Three of the seven different β subunits are fully processed during assembly and maturation of the protein with release of the amino-terminal nucleophile, Thr1, in the active sites of the β1, β2 and β5 subunits. Mutational studies in yeast have shown that these three β subunits are responsible for the three major proteolytic activities of the eukaryotic proteasome against small chromogenic substrates and a large protein, respectively [10–12], that is, β1 for the post-glutamyl peptide hydrolytic (PGPH), β2 for the trypsin-like and β5 for the chymotrypsin-like activity.

Specific modulation of these activities with reversible and irreversible inhibitors is essential for a better understanding of the mechanism of action of this enzyme in substrate degradation and thus in cytosolic protein breakdown. For this purpose, various reversible and irreversible synthetic inhibitors have been proposed (for a recent review, see [13]). Besides the known peptidyl α′β′-epoxyketone [14], peptidyl chloromethyl ketone and peptidyl diazomethyl ketone irreversible inhibitors [15], 3,4-dichloroisocoumarin [16,17] was found to to react covalently with Thr1 in the active site 18,19] and the microbial natural product lactacystin [20] was shown to react with the same site via its active *clasto*-lactacystin-β-lactone intermediate [21,22]. Although lactacystin still exhibits partial inhibition of both the PGPH and trypsin-like activities [20,23], significantly more selective inhibitors for the chymotrypsin-like activity

were obtained with peptidyl vinylsulfones [24,25]. For a reversible inhibition of mammalian proteasomes, a series of peptide aldehydes and peptide boronic acids was synthesized, with the main focus on the chymotrypsin-like activity (for a recent review, see [26]). Cross-reaction of the synthetic inhibitors with other proteases is known to occur, but, surprisingly, even the natural product lactacystin was found to inactivate cathepsin A as well as the proteasome [27].

Previous studies determined that the treatment of mammalian [28,29] and yeast [12] proteasomes with large excesses of the thiol reagent N-ethylmaleinimide (NEM) leads to selective inhibition of the trypsin-like activity. Because of the high reactivity of NEM, at least 17 sites per enzyme particle were found to be modified, so the experiments did not identify the essential residues for the proteolytic activity. The crystal structure of yeast 20S proteasome revealed that a cysteine residue is located near to the β2 active site, Cys118 of the β3 subunit, which protrudes with its sidechain into the S3 subsite of this active site [9]. This cysteine residue is conserved among the known primary structures of the β3 subunits of eukaryotic proteasomes; the observed inactivation of the trypsin-like activity of the mammalian and yeast proteasomes might, therefore, indeed derive from the chemical modification of this thiol function if recognition and binding of the substrate is prevented by the cyclic N-ethyl-succinimidylthio moiety in the S3 subsite.

In the present study, we have analyzed the possibility of exploiting the Cys118 thiol function for the development of new inhibitors that selectively address the active site of the β2 subunit and, therefore, its trypsin-like activity. We had to use the crystal structure of yeast proteasome [9] as a basis for the design of these inhibitors, because no structural data of the mammalian proteasomes are available so far. As outlined schematically in Figure 1, the cysteine residue in the S3 subsite was used to anchor peptide aldehyde inhibitors via a thiol-reactive 'handle' in close proximity to the Thr1 residue of the β2 active site for inactivation of the amino-terminal nucleophile by a covalent hemiacetal bond. With this inhibitor design, the basic principle of multivalency [30,31] was applied in a new version, in which specific recognition of peptide aldehydes adapted in their structure to the S subsites leads to a covalent grafting near the active site and therefore to an increase in the concentration around the active site to values that could make the inhibition practically irreversible.

Results

Structure-based design of maleinimide-functionalized peptide aldehydes

The mode of binding of the peptide aldehyde Ac-Leu–Leu–Nle-H (where Nle = norleucine) to the active-site of the β2 subunit via hemiacetal linkage to the Oγ of Thr1 is well established by the X-ray structure of the yeast proteasome–inhibitor adduct [9]. We used this structure for modelling experiments in which the Ac-Leu moiety of the bound inhibitor was deleted and replaced by a maleinimide group as the thiol-reactive handle. This group was positioned as a P3 residue into the S3 subsite in interacting distance from the Cys118 thiol function. From the kinetic point of view, upon recognition and binding of the P1–P2 moiety by the active site, the reaction of the maleinimide group with the Cys118 thiol should occur immediately, if a spacer of the correct size and properties is used. The ethylene moiety was selected as the spacer (Figure 1) because it was predicted that, as ethylene is relatively small, it would restrict the movements of the maleinimide group but allow the rotational motion required for an optimal adaptation to the reactive thiol group. Because of the unique location of Cys118 in the S3 subsite of β2, such maleoyl-peptide aldehydes should act as classical reversible inhibitors at the β1 and β5 active sites with affinities related mainly to the sidechain properties of residues P1 and P2. The aldehydes exert a strong inactivation of the β2 active site, however, if the spacer of the bound dipeptide unit allows the maleinimide to react with with the thiol group or *vice versa* if formation of the succinimidylthio group allows optimal fitting of the dipeptide unit into the S1–S2 subsites.

Figure 1

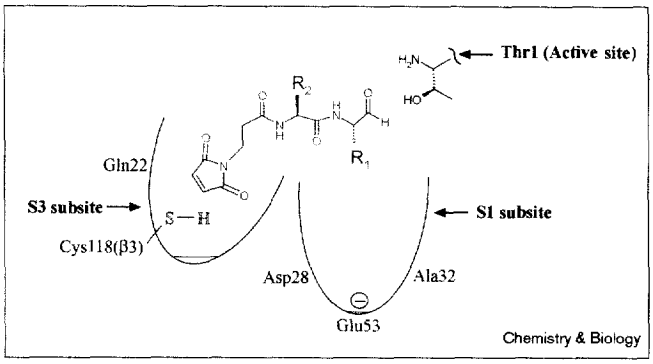

A schematic representation of the S subsites of the β2 active site of the yeast 20S proteasome as derived from the X-ray structure of the Ac-Leu–Leu–Nle-H/proteasome adduct [9] with maleoyl-β-alanyl-dipeptide aldehydes as potential inhibitors.

Synthesis of maleoyl-β-alanyl-dipeptide aldehydes

For a detailed analysis of the inhibition of the three major activities of the proteasome by maleinimide-functionalized dipeptide aldehydes, the three compounds listed in Table 1 were synthesized. For the synthesis of the maleoyl-β-alanyl-dipeptide aldehyde derived from the calpain inhibitor I, Mal-βAla–Leu–Nle-H (**2**), we made use of the intermediate H-Leu–Nle-Sc from our previously reported synthesis of Ac-Leu–Leu–Nle-H (**1**) [32] with the aldehyde protected as semicarbazone (Sc). Reaction with Mal-βAla-OSu (where OSu = N-hydroxysuccinimide ester) [33] followed by mild-acid treatment in presence of formaldehyde to drive the

Table 1

Synthetic maleoyl-β-alanyl-dipeptide aldehydes as potential inhibitors of the β2 active site of eukaryotic proteasomes.

Inhibitor	Structure
Mal-βAla–Leu–Nle-H (**2**)	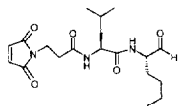
Mal-βAla–Val–Lys-H (**3**)	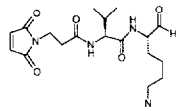
Mal-βAla–Val–Arg-H (**4**)	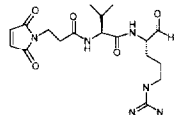

Figure 2

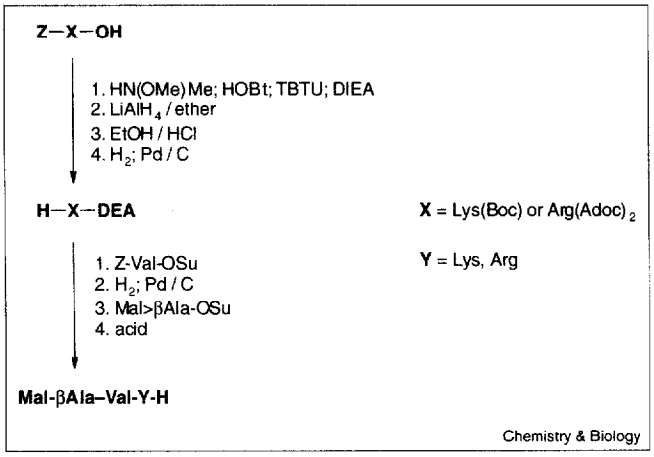

Synthesis of maleoyl-β-alanyl-dipeptide aldehydes.

semicarbazone hydrolysis to completion, led to compound **2** as an analytically well-characterized product.

For the synthesis of the peptide aldehydes **3** and **4**, Z-Lys(Boc)-OH and Z-Arg(Adoc)$_2$-OH were converted to the corresponding Weinreb amides that were then reduced with $LiAlH_4$ to produce the related aldehydes, as outlined in Figure 2. These were protected as diethyl acetals for the further amino-terminal elongation steps to the dipeptides and finally to the maleoyl derivatives. Upon acid treatment of the fully protected intermediates, the maleoyl-β-alanyl-dipeptide aldehydes **3** and **4** were isolated as hydrochloride and trifluoroacetate, respectively, and as stable compounds upon storage in the cold.

Inhibition of yeast proteasome with maleoyl-dipeptide aldehydes

To compare the inhibitory potencies of maleoyl-β-alanyl-dipeptide aldehydes with inactivation by the simple thiol reagent NEM, the yeast proteasome was incubated with NEM at concentrations ranging from 1 μM to 1 mM. As expected from previous findings in mammalian [28,29] and yeast [12] proteasomes, the PGPH and chymotrypsin-like activities are not affected by NEM at concentrations up to 100 μM (data not shown). Conversely, as shown in Figure 3a, incubation of the proteasome with 1 μM or 10 μM NEM leads to a time-dependent weak, but well-detectable reduction of the trypsin-like activity. At 100 μM and, in an even more pronounced manner, at 1 mM NEM concentration significantly faster inactivation is observed which reaches a plateau value of approximately 10% residual activity after 1 h and 40 min incubation, respectively. These results are in full agreement with earlier findings [12,28,29]. The residual activity of about 10% may be attributed to partial access of the substrate to the S3-blocked β2 active site. More probable, however, is the non-specific cleavage of the trypsin-substrate at the other two active sites of the multicatalytic protease, as a residual trypsin-like activity of 15% was also determined for a β2 subunit Thr1→Ala mutant of yeast proteasome [10]. This would suggest that at high concentrations NEM is capable of inactivating the active site of the β2 subunit almost completely by modifying the adjacent Cys118 residue of the β3 subunit. Although maleinimides are known for their very fast and quantitative reaction with thiols [34,35], the slow and highly concentration-dependent kinetics of inactivation can only be explained by a strongly impeded diffusion of the reagent into the inner chamber of the proteasome.

Ac-Leu–Leu–Nle-H inhibits the chymotryptic activity of the yeast proteasome with high potency (IC_{50} = 2.1 μM) and very weakly inhibits both the PGPH and trypsin-like activities (Table 2). Correspondingly, both the potency and the time course of inactivation of the yeast proteasome by the related maleoyl compound **2** were expected to be similar to that by NEM. As shown in Figure 3b, at just 100 μM concentration of compound **2** the trypsin-like activity is, however, totally blocked after 30 min incubation. When crystals of the proteasome from *Thermoplasma acidophilum* [36] and *S. cerevisiae* [9] are soaked with 5mM calpain inhibitor I, all active sites are occupied by the tripeptide aldehyde, confirming the relatively unspecific substrate, and therefore inhibitor, recognition properties of the single active sites of the proteasomes. This unspecific recognition of the maleoyl-dipeptide aldehyde **2** by the β2 active site could explain the significantly higher inactivation potency of this compound than that of NEM. Moreover, at 100 μM concentration inhibitor **2** apparently competes very efficiently with the trypsin substrate Bz-Phe–Val–Arg-AMC (where AMC = 7-amido-4-methyl-coumarin) for binding to

Figure 3

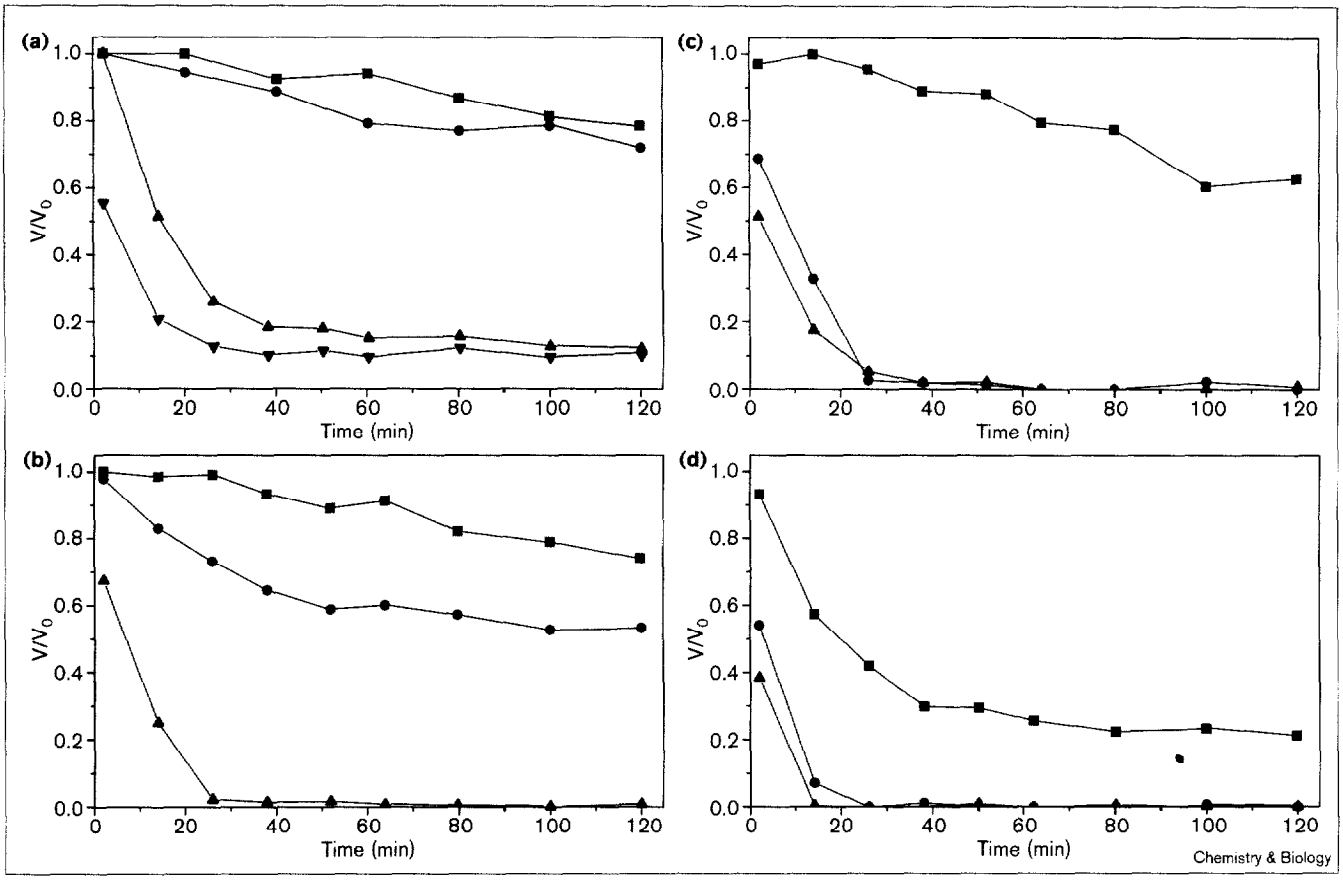

Time dependency of inhibition of yeast proteasome by **(a)** NEM, **(b)** Mal-βAla–Leu–Nle-H (**2**), **(c)** Mal-βAla–Val–Lys-H (**3**), **(d)** Mal-βAla–Val–Arg-H (**4**) at 1 μM (■), 10 μM (●), 100 μM (▲) and 1 mM (▼).

the β1 and β5 sites, thus leading to the quantitative suppression of substrate hydrolysis. As expected from the inhibitory properties of Ac-Leu–Leu–Nle-H (Table 2), the related compound **2** does not inhibit the proteasome's PGPH activity, but surprisingly it doesn't even inhibit the chymotryptic activity when these activities are measured with the 'specific' substrates Z-Leu–Leu–Glu-βNA and Suc-Leu–Leu–Val–Tyr-AMC, respectively. Replacement of the Ac-Leu portion of the calpain inhibitor-I with the Mal-βAla moiety therefore strongly reduces the affinity of the inhibitor for the β5 chymotryptic site. The strong effect of hydrophobic P3 residues on inhibition of the chymotryptic activity of the proteasome is well established [37]. The time dependency of inactivation of the yeast proteasome by Mal-βAla–Leu–Nle-H (**2**), shown in Figure 3b, raises the question of whether or not peptidic compounds penetrate the proteasome barrel faster than even smaller, but nonpeptidic compounds like NEM because there is such a weak recognition of the Leu–Nle-H moiety by the subsites of the β2 active site to direct the reaction of the maleoyl group with Cys118 of the S3 subsite.

Conversely, the incorporation of a basic residue into position P1 of the dipeptide aldehyde moiety was expected to greatly facilitate this recognition process and thus also facilitate binding to the β2 active site. Indeed the inactivation potency of Mal-βAla–Val–Lys-H (**3**) is significantly enhanced, with an IC_{50} value of 3.4 μM (Table 2), compared with compound **2** (IC_{50} = 13 μM). With 10 μM inhibitors, the trypsin-like activity is switched off and the time course of inactivation (Figure 3c) again shows full

Table 2

Inhibition of the PGPH, trypsin- and chymotrypsin-like activities of yeast proteasome by maleoyl-β-alanyl-dipeptide aldehydes.

Inhibitor	PGPH	Trypsin-like	Chymotrypsin-like
Ac-Leu–Leu–Nle-H	>100	>100	2.1
Mal-βAla–Leu–Nle-H	>100	13	>100
Mal-βAla–Val–Lys-H	>100	3.4	>100
Mal-βAla–Val–Arg-H	>100	0.5	>100

Figure 4

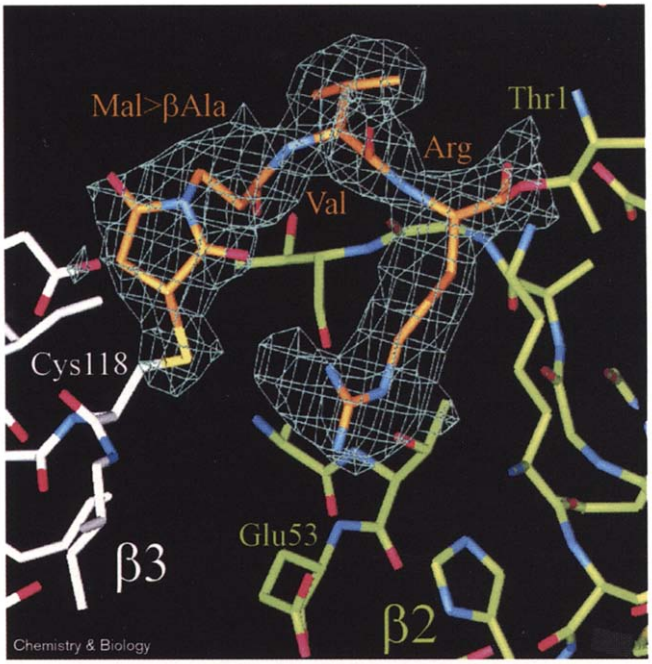

Model and electron-density map of the yeast 20S proteasome/Mal-βAla–Val–Arg-H (4) adduct. The electron density map was calculated with phases of the free enzyme structure and contoured around the inhibitor molecule at 2s cutoff. The model parts are marked with different colours for their carbon atoms: green for β2, white for β3 and yellow for the inhibitor.

inactivation after about 30 min incubation at inhibitor concentrations higher than the IC_{50} value, indicating that this time interval is related to the slow k_{on} rate of the inhibition process, which is dominated by the hampered diffusion into the proteasome barrel.

By replacing the lysine with arginine as P1 residue, an additional improvement in the inhibitory potency ($IC_{50} = 0.5\ \mu M$) is observed and, within the limits of error of the assay system, again about 30 min are required for full inactivation of the proteasome (Figure 3d). Given that a 100-fold dilution of the inhibited enzyme was not restoring trypsin-like activity, the working assumption of a covalent linkage of the inhibitor to Cys118 was confirmed.

The presence of three active sites of limited substrate specificity and the difficult access of molecules into the inner chamber of the barrel-shaped multicatalytic protease make kinetic evaluation of the inhibition data difficult and complex [38]. Moreover, in the present case irreversible linkage of the inhibitors in the *pros*-position to the active site and reversible hemiacetal linkage of the aldehyde to the active-site Thr1 adds further complication. The inhibitory potencies of the maleoyl-β-alanyl-dipeptide aldehydes were therefore compared with each other in terms of the IC_{50} values that were determined for the PGPH, chymotrypsin- and trypsin-like activities (Table 2).

X-ray structure of the proteasome–inhibitor 4 adduct

The binding mode of this new class of inhibitors was determined using X-ray structural analysis of the yeast proteasome–inhibitor **4** adduct at 2.5 Å resolution. As shown in Figure 4, the electron-density map of the crystals soaked with Mal-βAla–Val–Arg-H is well-defined and clearly depicts the structure of the inhibitor bound to the β2 active site. The β1 and β5 active sites are not occupied by this inhibitor, in contrast to Ac-Leu–Leu–Nle-H, which, in crystals of the yeast proteasome, is bound to all three active sites. The latter finding is in full agreement with the low inhibition of the chymotrypsin-like and PGPH activities of the proteasome by Mal-βAla–Val–Arg-H. The inhibitor is covalently linked at the carboxyl terminus to the Oγ of Thr1 via hemiacetal bond formation, whereby the resulting hydroxyl group is hydrogen bonded to the backbone CO of Gly47. The arginine sidechain is deeply inserted into the S1 pocket forming a salt bridge between the guanidino group and the carboxylate of Glu53. This interaction is reinforced by the Asp28 carboxylate and by an additional hydrogen bond to the carbonyl oxygen of Ala32. The sidechain of Glu53 is visibly shifted from its original position to form the salt bridge. Valine was selected as the P2 residue, in analogy to the substrate used to measure the inhibition of the trypsin-like activity; although already from the X-ray structure of the proteasome/Ac-Leu–Leu–Nle-H adduct it was known that the S2 subsite is shallow and does not have particular binding preferences [9]. The sidechain of valine as the P2 residue points to the bulk water and a hydrogen-bonding network is established between the peptide backbone of the inhibitor and the substrate-binding cleft of the β2 active site. In fact, the valine CO and NH are hydrogen bonded to Thr21 NH and CO, respectively, and the β-alanine CO to Ala49 NH. The S→C distance was measured after manual fitting of the inhibitor into the electron-density map calculated from the model of the enzyme. The S→C distance is 2.15 Å and therefore reasonably close to the distance of a single S–C bond (1.82 Å), which indicates covalent thiosuccinimidyl linkage of the inhibitor to Cys118 of the β3 subunit. The thiol addition to the maleinimide double bond occurs at only one of the two possible carbon atoms in the defined *R*-configuration, and the resulting thiosuccinimidyl ring is held into juxtaposition by hydrogen-bonding interactions between the imido group and the Ser20 hydroxyl function, and between the succinimide carbonyl distal to the thioether bond and the sidechain amide of Gln22. Given that a well-defined electron-density map was even obtained for the ethylene spacer, its motion is apparently highly restricted indicating an optimal length and sufficient flexibility to place the maleinimide group into interacting distance with the cysteine thiol for adduct formation.

Discussion

Lactacystin, a microbial natural product, irreversibly inhibits the chymotrypsin-like activity of mammalian proteasomes [20]. The X-ray structure of the yeast proteasome–lactacystin adduct revealed the presence of this inhibitor covalently linked via an ester bond to the Oγ of Thr1 in the β5 active site, where a dense network of hydrogen bonds and hydrophobic interactions hold the molecule in position to allow its high degree of selectivity [9]. The chymotrypsin-like activity is completely switched off with lactacystin, but partial inhibition of the PGPH and tryptic activities is also observed [20,23]. Very recently, attempts have been made to develop selective peptidyl vinylsulfone inhibitors [24,25]. A high degree of selectivity was obtained for the β5 active site, whereas selective inhibition of the β1 and β2 active sites was less successful. Conversely, the maleoyl dipeptide aldehyde Mal-βAla–Val–Arg-H (**4**) exclusively inactivates the β2 active site of the proteasome and therefore the associated trypsin-like activity switched off.

The inactivation potencies of the maleoyl-dipeptide aldehydes were found to depend strongly upon the sidechain of the carboxy-terminal amino acid aldehyde. This finding supports the specific recognition of this portion of the molecule by the enzyme S1 subsite; conversion to the hemiacetal is the primary event, followed by juxtaposition of the maleinimide group at the S3 subsite for reaction with the thiol function of Cys118 and therefore for irreversible grafting of the inhibitor to this active site. This mechanism of inactivation could also explain why, in contrast to NEM, the X-ray structure revealed only one such molecule bound to the proteasome, despite the presence of multiple accessible cysteine residues and the soaking of the crystals with a 100-fold excess of the maleoyl compound **4**.

Significance

Eukaryotic proteasomes are involved in the degradation of a multitude of proteins and peptides and therefore only a limited substrate specificity characterizes their active sites in the β1, β2 and β5 subunits responsible for the post-glutamyl-peptide hydrolytic, trypsin-like and chymotrypsin-like activities, respectively. This makes substrate-based design of selective inhibitors extremely difficult. The unique location of a cysteine residue, Cys118 of β3, in *pros*-position to the active site of the β2 subunit of yeast proteasome was used for the design of a new type of inhibitor based on the covalent linkage of peptide aldehydes to the thiol function. A fully selective inactivation of the β2 active site of the yeast proteasome was achieved by exploiting the trypsin-like preference of the S1 subsite for basic residues and the high reactivity of maleinimide towards thiols. Given that Cys118 is highly conserved among the known primary structures of mammalian proteasomes, the new inhibitor could represent a powerful new tool for studying the mechanism of substrate degradation of these complex proteases. The only limitation for the use of this inhibitor is that it shows reactivity towards all types of thiols.

Materials and methods

All solvents and reagents used in the synthesis were of the highest quality commercially available, and when required were further purified and dried by standard methods. Thin-layer chromatography (TLC) silica gel 60 plates were from Merck AG (Darmstadt, Germany) and compounds were visualized with the chlorine/tolidine or permanganate reagent. Analytical high-performance liquid chromatography (HPLC) was performed on Nucleosil 100/C18 columns (Macherey-Nagel, Düren, Germany) using linear gradients of MeCN/2% H_3PO_4 from 5:95 to 80:20 (A) or MeCN/2% H_3PO_4 from 30:70 to 80:20 (B) in 30 min. Preparative HPLC was carried out on Nucleosil RP 18 (Macherey-Nagel, Düren, Germany) with linear gradients of MeCN/water from 5:95 to 50:50 in 90 min. Fast-atom bombardment (FAB)–MS spectra were recorded on a Finnigan MAT 900 and matrix-assisted laser desorption ionization–time-of-flight (MALDI–TOF)–MS on a Bruker Relflex III-TOF MS (Bruker-Franzen, Bremen, Germany).

The substrates Z-Leu–Leu–Glu-βNA, Bz-Phe–Val–Arg-AMC and Suc-Leu–Leu–Val–Tyr-AMC were purchased from Bachem (Heidelberg, Germany). Proteasome from *S. cerevisiae* was prepared as described previously [9] and the synthesis of Ac-Leu–Leu–Nle-H (**1**) and H-Leu–Nle-Sc trifluoroacetate was reported elsewhere [32].

*Synthesis Mal-βAla–Leu–Nle-H (**2**)*

Mal-βAla–Leu–Nle-Sc. To a solution of H-Leu-Nle-Sc trifluoroacetate (90 mg; 0.23 mmol) and diisopropylethylamine (DIEA) (39 µl; 0.23 mmol) in 1 ml dimethylformamide (DMF) was added Mal–βAla-OSu [33] (66 mg; 0.25 mmol) in 1 ml DMF. After 20 h stirring at room temperature the solvent was removed under reduced pressure and the residue distributed between AcOEt and water. The aqueous phase was extracted twice with AcOEt and the combined organic layers were washed with 5% $KHSO_4$, 5% $NaHCO_3$ and water, and dried over $MgSO_4$. Evaporation of the solvent gave white crystals; yield: 68 mg (69%); TLC ($CHCl_3$/*i*PrOH, 8:1) R_f 0.6; HPLC (gradient A): t_R 20.1 min.

Mal-βAla–Leu–Nle-H. Mal-βAla–Leu–Nle-Sc (65 mg; 0.15 mmol) was dissolved in a mixture of 3 ml MeOH, 0.6 ml AcOH and 0.6 ml of 37% formaldehyde. After 2.5 h the solvent was evaporated and the oily residue was purified by preparative HPLC. Fractions containing pure product were collected and lyophilised; yield: 14 mg (25%); HPLC (gradient A): t_R 16.2 min; FAB-MS: $m/z = 380$ $[M+H^+]$; $M_r = 379.2$ calc'd for $C_{19}H_{29}N_3O_5$.

*Synthesis of Mal-βAla–Val–Lys-H (**3**)*

Z-Lys(Boc)-N(OMe)Me. To Z-Lys(Boc)-OH (6.07 g; 16 mmol), TBTU (5.12 g; 16 mmol), HOBt (2.15 g; 16 mmol) and DIEA (2.73 ml; 16 mmol) in 100 ml CH_2Cl_2 was added at 0°C HN(OMe)Me (1.71 g; 18 mmol) and DIEA (2.99 ml; 18 mmol) in 50 ml CH_2Cl_2. After 15 h stirring at room temperature the solvent was evaporated and the residue distributed between AcOEt and 5% $KHSO_4$. The aqueous layer was extracted twice with AcOEt and the combined organic layers were washed with 5% $KHSO_4$, 5% $NaHCO_3$ and water. The solution was dried over $MgSO_4$ and after removal of the solvent a yellowish oil was obtained; yield: 6.37 g (94%); TLC (AcOEt/petroleum ether, 2:1): R_f 0.7; HPLC (gradient A): t_R 27.3 min; FAB-MS: $m/z = 424$ $[M+H^+]$; $M_r = 423.2$ calc'd for $C_{21}H_{33}N_3O_6$.

Z-Lys(Boc)-H. To an ice-cold solution of Z-Lys(Boc)N(OMe)Me (3.36 g; 7.8 mmol) in 90 ml of dry argon saturated ether, $LiAlH_4$ (0.38 g; 10 mmol) was added in small portions. After stirring at room temperature for 1 h the mixture was cooled again to 0°C, and the reaction was quenched with 0.1 M HCl (55 ml). The aqueous phase was extracted twice with methyl *tert*-butyl ether and the combined organic layers were washed with 5% $KHSO_4$, 5% $NaHCO_3$ and water, and dried over $MgSO_4$. The solution

was taken to dryness; yield: 2.57 g (95%) of yellowish oil; TLC (AcOEt/petroleum ether, 2:1): R_f 0.8; HPLC (gradient A): t_R 24.4 min; FAB-MS: $m/z = 365$ $[M+H^+]$; $M_r = 364.2$ calc'd for $C_{19}H_{28}N_2O_5$.

Z-Lys(Boc)-DEA. Z-Lys(Boc)-H (2.74 g; 7.5 mmol) was dissolved under an argon atmosphere in 40 ml of 0.5% HCl in dry EtOH at −40°C. After 20 h at 4°C sodium acetate (3 g; 38 mmol) was added followed by 100 ml water. The solution was concentrated to 50 ml and extracted with AcOEt. The combined organic layers were washed with water, dried over $MgSO_4$ and evaporated. The crude product was chromatographed on silica gel with petroleum ether/AcOEt (3:2). Upon concentration of the pure fractions and precipitation with hexane the product was obtained as white needles; yield: 2.20 g (67%); TLC (AcOEt/petroleum ether, 1:1): R_f 0.8; HPLC (gradient A): t_R 29.8 min; FAB-MS: $m/z = 439$ $[M+H^+]$; $M_r = 438.3$ calc'd for $C_{23}H_{38}N_2O_6$.

H-Lys(Boc)-DEA. Z-Lys(Boc)-DEA (1.0 g; 2.3 mmol) was hydrogenated in 100 ml of 95% MeOH over Pd/C (10%). After 1 h the catalyst was filtered off and the filtrate evaporated to give a colourless oil; yield: 0.55 g; (79%); TLC ($CHCl_3$/MeOH/AcOH; 3:1:0.1): R_f 0.7; HPLC (gradient A): t_R 17.7 min; FAB-MS: $m/z = 305$ $[M+H^+]$; $M_r = 304.2$ calc'd for $C_{15}H_{32}N_2O_4$.

Z-Val–Lys(Boc)-DEA. Z-Val-OH (0.52 g; 1.7 mmol), EDC (0.31 g; 1.6 mmol), HOBt (0.243 g; 1.8 mmol) and DIEA (0.28 ml; 1.8 mmol) were dissolved in 10 ml DMF, and at 0°C a solution of H-Lys(Boc)-DEA (0.52 g; 1.7 mmol) in 5 ml DMF was added. After stirring overnight at room temperature the solvent was removed and the residue distributed between AcOEt and 5% $KHSO_4$. The organic layer was washed with 5% $KHSO_4$, 5% $NaHCO_3$ and water, and dried over $MgSO_4$. The solution was concentrated to small volume and the product was precipitated with hexane; yield: 0.78 g (85%) of white crystals; TLC ($CHCl_3$/MeOH/AcOH; 14:1:0.1): R_f 0.6; HPLC (gradient A): t_R 29.3 min; FAB-MS: $m/z = 538$ $[M+H^+]$; $M_r = 537.3$ calc'd for $C_{28}H_{47}N_3O_7$.

H-Val–Lys(Boc)-DEA. N^{α}-Deprotection was performed as described for H-Lys(Boc)-DEA and the product was isolated by precipitation from AcOEt with diisopropyl ether; yield: 0.43 g (75%) of white crystals; TLC ($CHCl_3$/MeOH/AcOH, 14:1:0.1): R_f 0.4; HPLC (gradient A): t_R 20.5 min; FAB-MS: $m/z = 404$ $[M+H^+]$; $M_r = 403.3$ calc'd for $C_{20}H_{41}N_3O_5$.

Mal-βAla–Val–Lys(Boc)-DEA. To a solution of H-Val–Lys(Boc)-DEA (0.21 g; 0.51 mmol) in 2 ml DMF Mal-βAla-OSu (0.15 g; 0.56 mmol) was added and the reaction mixture was worked up as described for Mal-βAla-Leu-Nle-Sc. The product was precipitated from AcOEt with hexane; yield: 0.20 g (71%); TLC ($CHCl_3$/MeOH/AcOH, 14:1:0.1): R_f 0.8; HPLC (gradient A): t_R 24.7 min; FAB-MS: $m/z = 555$ $[M+H^+]$; $M_r = 554.3$ calc'd for $C_{27}H_{46}N_4O_8$.

Mal-βAla–Val–Lys·HxHCl. Mal–βAla–Val–Lys(Boc)-DEA (75 mg; 0.14 mmol) was reacted in 3 ml MeCN with 3 M HCl (3 ml) at 0°C for 1 h. Then the solvent was removed and the crude product purified by preparative HPLC. Fractions containing pure product were collected and lyophilised; yield: 23 mg (41%); TLC ($CHCl_3$/MeOH/AcOH, 1:1:0.1): R_f 0.4; HPLC (gradient A): t_R 6.2 min; FAB-MS: $m/z = 381$ $[M+H^+]$; $M_r = 380.2$ calc'd for $C_{18}H_{28}N_4O_5$.

*Synthesis of Mal-βAla–Val–Arg-H(**4**)*

Z-Arg(Adoc)$_2$-DEA. The Weinreb amide was obtained as described for Z-Lys(Boc)-N(OMe)Me (yield: 97%; TLC ($CHCl_3$/MeCN/AcOH, 10:1:0.1): R_f 0.7; HPLC (gradient B): t_R 26.6 min) and then reduced to the aldehyde as reported for Z-Lys(Boc)-H [yield: 97%; TLC ($CHCl_3$/MeCN/AcOH, 10:1:0.1) R_f 0.8; HPLC (gradient B): t_R 25.3 min]. Protection of the aldehyde was performed as described for the Lys derivative; yield: 69%; TLC (petroleum ether/AcOEt, 10:3): R_f 0.7; HPLC (gradient B): t_R 29.7 min; MALDI-TOF-MS: $m/z = 723$ $[M+H^+]$; $M_r = 722.4$ calc'd for $C_{40}H_{58}N_4O_8$.

Mal-βAla–Val–Arg(Adoc)$_2$-DEA. The title compound was synthesized as described for the related Lys derivative in 44% yield over the four steps; TLC ($CHCl_3$/MeOH/AcOH, 15:1:0.1): R_f 0.4; HPLC (gradient B): t_R 26.5 min.

Mal-βAla–Val–Arg·HxTFA. Mal-βAla–Val–Arg(Adoc)$_2$-DEA (75 mg; 0.09 mmol) was dissolved in 95% TFA. After 1 h methyl *tert*-butyl ether was added, the precipitate collected by centrifugation and purified by preparative HPLC. Fractions containing pure product were pooled and lyophilised to give a white powder; yield: 12 mg (32%); TLC ($CHCl_3$/MeOH/AcOH, 1:1:0.1): R_f 0.8; HPLC (gradient A): t_R 8.8 min; FAB-MS: $m/z = 409$ $[M+H^+]$; $M_r = 408.2$ calc'd for $C_{18}H_{28}N_6O_5$.

Proteasome assay

For the determination of IC_{50} values a solution of yeast proteasome in Tris buffer (pH 7.5; 450 µl; 6.67 nM for PGPH, 5.56 nM for trypsin-like and 1.11 nM for chymotrypsin-like activity) was incubated at 37°C with the inhibitors at varying concentrations. After 1 h 5 µl of a 0.2 M solution of mercaptoethanol was added followed by the fluorogenic substrates for PGPH (Z-Leu–Leu–Glu-βNA, 40 µM), trypsin-like (Bz-Phe–Val–Arg-AMC, 8 µM) and chymotrypsin-like (Suc-Leu–Leu–Val–Tyr-AMC, 8 µM) assays. The substrates were previously dissolved in the same Tris-buffer with a minimum amount of DMSO, and the final volume of the samples was 500 µl. Fluorescence excitation/emission wavelengths were 360 nm/460 nm for AMC and 355 nm/410 nm for βNA. The rates of hydrolysis were monitored by the fluorescence increase and the initial linear portions of curves (100–300 s) were used to calculate the IC_{50} values.

The experimental procedure for measuring the time-dependency of inhibition of the trypsin-like activity was performed as described above, except that the incubation time of the enzyme with the inhibitors was varied from 2 to 120 min.

X-Ray structure analysis

Crystals of 20S proteasomes from *S. cerevisiae* were grown in hanging drops at 24°C as described previously [9]. The protein concentration used for crystallization was 40 mg/ml in 10 mM Tris–HCl (pH 7.5) and 1 mM EDTA. The drops contained 4 µl protein and 2 µl reservoir solution with 30 mM magnesium acetate, 100 mM morpholino-ethane-sulphonic acid (pH 6.5) and 11% MPD. The final inhibitor concentration was 5 mM and crystals were soaked for 12 h.

The space group belongs to $P2_1$ with cell dimensions of $a = 134.72$ Å, $b = 300.51$ Å, $c = 144.25$ Å and $\beta = 112.91°$. Data to 2.5 Å were collected using synchrotron radiation with $\lambda = 1.1$ Å on the BW6-beamline at the DESY-Centre/Hamburg/Germany. Crystals were soaked in a cryoprotecting buffer (30% MPD, 28 mM magnesium acetate, 100 mM morpholino-ethane-sulfonic acid (pH 6.9) and frozen in a stream of cold nitrogen gas at 90 K (Oxford Cryo Systems). X-ray intensities were evaluated by using the MOSFILM program package (version 5.3) and data reduction was performed with CCP4. The anisotropy of diffraction was corrected by an overall anisotropic temperature factor by comparing observed and calculated structure amplitudes using the program X-PLOR [39]. A total of 863058 reflections yielding 345223 unique reflections (96.1% completness) was collected. The corresponding R-merge was 6.4% at 2.5 Å resolution (26.9% for the 2.6–2.5 Å resolution shell). Electron density was averaged 10 times over the twofold noncrystallographic symmetry axis using the program package MAIN [40]. Conventional crystallographic rigid body, positional and temperature factor refinements were carried out with XPLOR using the yeast 20S proteasome structure [9] as starting model. Model building was carried out with the program FRODO [41]. The structure was refined to a R-factor of 24.4% (free R-factor = 29.2%) with rms-deviations from target values of 0.011 Å for bonds and 1.395° for angles [42]. Modelling experiments were performed using the coordinates of yeast 20S proteasome with MAIN [40].

Acknowledgements

The study was supported by the Deutsche Forschungsgemeinschaft (SFB 469; grants A1 and A2). The help of G.B. Bourenkow and H. Bartunik, Max-Planck Arbeitsgruppen, Hamburg, with data collection is gratefully acknowledged.

References

1. Goldberg, A.L., Stein, R. & Adams, J. (1995). New insights into proteasome function – from archaebacteria to drug development. *Chem. Biol.* **2**, 503-508.
2. Hochstrasser, M. (1995). Ubiquitin, proteasomes, and the regulation of the intracellular protein degradation. *Curr. Opin. Cell Biol.* **7**, 215-223.
3. Coux, O., Tanaka, K. & Goldberg, A.L. (1996). Structure and functions of the 20S and 26S proteasomes. *Annu. Rev. Biochem.* **65**, 801-847.
4. Stock, D., Nederlof, P.M., Seemüller, E., Baumeister, W., Huber, R. & Löwe, J. (1996). Proteasome: from structure to function. *Curr. Opin. Biotech.* **7**, 376-385.
5. Chen, P. & Hochstrasser, M. (1995). Biogenesis, structure and function of the yeast 20S proteasome. *EMBO J.* **14**, 2620-2630.
6. Groettrup, M., Soza, A., Kuckelkorn, U. & Kloetzel. P.M. (1996). Peptide antigen production by the proteasome: complexity provides efficiency. *Immunol. Today* **17**, 429-435.
7. Hilt, W. & Wolf, D.H. (1996). Proteasomes: destruction as a programme. *Trends Biochem. Sci.* **21**, 96-102.
8. Baumeister, W., Walz, J., Zühl, F. & Seemüller, E. (1998). The proteasome: paradigm of a self-compartmentalizing protease. *Cell* **92**, 367-380.
9. Groll, M., *et al.*, & Huber, R. (1997). Structure of 20S proteasome from yeast at 2.4 Å resolution. *Nature* **386**, 463-471.
10. Heinemeyer, W., Fischer, M., Krimmer, T., Stachon, U. & Wolf, D.H. (1997). The active sites of the eukaryotic 20 S proteasome and their involvement in subunit precursor processing. *J. Biol. Chem.* **272**, 25200-25209.
11. Nussbaum, A.K., *et al.*, & Schild, H. (1998). Cleavage motifs of the yeast 20S proteasome β subunits deduced from digests of enolase I. *Proc. Natl Acad. Sci. USA* **95**, 12504-12509.
12. Arendt, C.S. & Hochstrasser M. (1997). Identification of the yeast 20S proteasome catalytic centers and subunit interactions required for active-site formation. *Proc. Natl Acad. Sci. USA* **94**, 7156-7161.
13. Lee, D.H. & Goldberg, A.L. (1998). Proteasome inhibitors: valuable new tools for cell biologists. *Trends Cell Biol.* **8**, 397-403.
14. Spaltenstein, A., *et al.*, & Crouch, R. (1996). Design and synthesis of novel protease inhibitors: tripeptide α′, β′-epoxyketones as nanomolar inactivators of the proteasome. *Tetrahedron Lett.* **37**, 1343-1346.
15. Reidlinger, J., Pike, A.M., Savory, P.J., Murray, R.Z. & Rivett, A.J. (1997). Catalytic properties of 26S and 20S proteasomes and radiolabeling of MB1, LMP7 and C7 subunits associated with trypsin-like and chymotrypsin-like activities. *J. Biol. Chem.* **272**, 24899-24905.
16. Pereira, M.E., Nguyen, T., Wagner, B.J., Margolis, J.W., Yu, B. & Wilk, S. (1992). 3,4-Dichloroisocumarin-induced activation of the degradation of beta casein by the bovine pituitary multicatalytic proteinase complex. *J. Biol. Chem.* **267**, 7949-7955.
17. Cardozo, C., Vinitsky, A., Hidalgo, M.C., Michaud, C. & Orlowski, M. (1992). A 3,4-Dichloroisocumarin-resistant component of the multicatalytic proteinase complex. *Biochemistry* **31**, 7373-7380.
18. Akopian, T.N., Kisselev, A.F. & Goldberg, A.L. (1997). Processive degradation of proteins and other catalytic properties of the proteasome from *Thermoplasma acidophilum*. *J. Biol. Chem.* **272**, 1791-1798.
19. Orlowski, M., Cardozo, C., Eleuteri, A.M., Kohanski, R., Kam, C.M. & Powers, J.C. (1997). Reactions of [^{14}C]-3,4-Dichloroisocumarin with subunits of pituitary and spleen multicatalytic proteinase complexes (proteasomes). *Biochemistry* **36**, 13946-13953.
20. Fenteany, G., Standaert, R.F., Lane, W.S., Choi, S., Corey, E.J. & Schreiber, S.L. (1995). Inhibition of proteasome activities and subunit-specific amino-terminal threonine modification by lactacystin. *Science* **268**, 726-731.
21. Dick L.R., *et al.*, & Stein R.L. (1997). Mechanistic studies on the inactivation of the proteasome by lactacystin in cultured cells. *J. Biol. Chem.* **272**, 182-188.
22. Corey, E.J., Reichard, G.A. & Kania, R. (1993). Studies on the total synthesis of lactacystin: an improved aldol coupling reaction and a beta-lactone intermediate in thiol ester formation. *Tetrahedron Lett.* **34**, 6977-6980.
23. McCormack, T.A., *et al.*, & Dick, L.R. (1998). Kinetic studies of the branched chain amino acid preferring activity of the 20S proteasome: development of a continuous assay and inhibition by tripeptide aldehydes and *clasto*-lactacystin β-lactone. *Biochemistry* **37**, 7792-7800.
24. Bogyo, M., McMaster, J.S., Gaczynska, M., Tortorella, D., Goldberg, A.L. & Ploegh, H. (1997). Covalent modification of the active site threonine of proteasomal beta subunits and the Escherichia coli homolog HslV by a new class of inhibitors. *Proc. Natl Acad. Sci. USA* **90**, 6629-6634.
25. Bogyo, M., Shin, S., McMaster, J.S. & Ploegh, H. (1998). Substrate binding and sequence preference of the proteasome revealed by active-site-directed affinity probes. *Chem. Biol.* **5**, 307-320.
26. Adams, J. & Stein, R. (1996). Novel inhibitors of the proteasome and their therapeutic use in inflammation. *Annu. Rep. Med. Chem.* **31**, 279-288.
27. Ostrowska, H., Omura, S., Wojcik, C. & Worowski, K. (1997). Lactacystin, a specific inhibitor of the proteasome, inhibits human platelet lysosomal cathepsin A-like enzyme. *Biochem. Biophys. Res. Comm.* **234**, 729-732.
28. Rivett, A.J. (1989). The multicatalytic proteinase. *J. Biol. Chem.* **264**, 12215-12219.
29. Dick, L.R., Moomaw, C.R., Pramanik, G.N., DeMartino, G.N. & Slaughter, C.A. (1992). Identification and localization of a cysteinyl residue critical for the trypsin-like catalytic activity of the proteasome. *Biochemistry* **31**, 7347-7355.
30. Spike, C.G. & Parry, R.W. (1953). Thermodynamics of chelation. I. The statistical factor in chelate ring formation. *J. Am. Chem. Soc.* **75**, 2726-2729.
31. Crothers, D.M. & Metzger, H. (1972). The influence of polyvalency on the binding properties of antibodies. *Immunochemistry* **9**, 341-357.
32. Schaschke, N., Musiol, H.-J., Assfalg-Machleidt, I., Machleidt, W., Rudolph-Böhner, S. & Moroder, L. (1996). Cyclodextrins as templates for the presentation of protease inhibitors. *FEBS Lett.* **391**, 297-301.
33. Romano, R., Bayerl, T.M. & Moroder, L. (1993). Lipophilic derivatization and its effect on the interaction of cholecystokinin (CCK) nonapeptide with phospholipids. *Biochim. Biophys. Acta* **1151**, 111-119.
34. Smyth, D.G. (1964). Reactions of *N*-ethylmaleimide with peptides and amino acids. *Biochem. J.* **91**, 589-595.
35. Wünsch, E., Moroder, L., Nyfeler, R., Kalbacher, H. & Gemeiner, M. (1985). Immunoassays of peptide factors.1. Synthesis of N^{α}-maleoyl-peptide derivatives. *Biol. Chem. Hoppe-Seyler* **366**, 53-61.
36. Löwe, J., Stock, D., Jap, B., Zwickl, P., Baumeister, W. & Huber, R. (1995). Crystal structure of the 20S proteasome from the archaeon *T. acidophilum* at 3.4 Å resolution. *Science* **268**, 533-539.
37. Palombella, V.J., Goldberg, A.L., Maniatis, T.P. & Rando O. (1995). Proteasome regulation of NF-κB activity. Patent WO 95/25533.
38. Stein, R.L., Melandri, F. & Dick, L. (1996). Kinetic characterization of the chymotryptic activity of the 20S proteasome. *Biochemistry* **35**, 3899-3908.
39. Brunger, A. (1992). *X-PLOR Version 3.1. A System for X-Ray Crystallography and NMR.*
40. Turk, D. (1992). Improvement of a program for molecular graphics and manipulation of electron-densities and its application for protein-structure determination. *Thesis*, Technische Universität München.
41. Jones, T.A. (1978). A graphic model building and refinement system for macromolecules. *J. Appl. Crystallogr.* **11**, 268-272.
42. Engh, R.A. & Huber, R. (1991). Accurate bond and angle parameters for X-ray protein structure refinement. *Acta Crystallogr. A* **47**, 392-400.

Because *Chemistry & Biology* operates a 'Continuous Publication System' for Research Papers, this paper has been published via the internet before being printed. The paper can be accessed from http://biomednet.com/cbiology/cmb – for further information, see the explanation on the contents pages.